Mitigating the Impact of Hand Sanitizer on the Spectral Signature of Finger Hypercubes

Emanuela Marasco and Yuanting Tao
Center for Secure Information Systems
George Mason University
Fairfax, VA 22030, USA
emarasco,ytao4@gmu.edu

2022 IEEE International Joint Conference on Biometrics (IJCB) | 978-1-6654-6394-2/22/$31.00 ©2022 IEEE | DOI: 10.1109/IJCB54206.2022.10008002

Abstract

The proposed study seeks to shed light on whether hand sanitizer impacts the spectral signature of hyperspectral fingerprint images. In the hyperspectral domain, fingerprint data consists of stacked images across pre-defined wavelengths. We process the central region of the fingerprint foreground through various techniques that account for baseline shifts in heterogeneous samples, different lighting conditions, and background noise. A non-parametric classifier-based two-sample test adapted to hyperspectral data is conducted to determine whether significant differences exist between samples acquired before and after applying hand sanitizer. Experiments were carried out on hyperspectral fingerprint images acquired from 50 subjects. For every image, 100 pixels selected for this analysis, with each pixel featured by 300 spectrum bands. Findings imply that, the spectra generated from the data without applying hand sanitizer differ from those obtained from the data collected after applying hand sanitizer. However, treating the spectra with proper pre-processing techniques significantly attenuates this issue.

1. Introduction

Hyperspectral imaging (HSI) is a powerful tool that could enable non-destructive analysis of spatially resolved spectral information of materials. HSI technology collects and processes information from across the electromagnetic spectrum to obtain the spectrum for each pixel in the image of a scene, with the purpose of finding objects, identifying materials, or detecting processes [1]. This advanced image processing technology coupled with pattern recognition can extract rich signals without the use of reagents. It holds great potential for security, forensics and medical applications. For example, HSI can improve understanding of the chemical character of latent fingerprints [2].

Since the COVID-19 global health emergency, multiple experts have mandated the use of hand sanitizers as a safety measure to fight against the coronavirus spread; thus, this product has become of common use [3]. Prajapati *et al.* have proved that the use of skin disinfectants deprives the skin from sebum and water hence causing skin dryness [4]. Hand sanitizers containing alcohol can also dissolve the lipid levels of the skin.

It is currently unknown whether and how hand sanitizers alter the spectral signature extracted from hyperspectral images. This paper seeks to answer to this question by approaching the problem through statistical machine learning. To the best of our knowledge, there is no prior research on detecting such an impact in the HSI domain nor established related work.

The contribution of this work is three-fold: *i)* design the process for finger hypercube segmentation, ROI extraction, and unfolding, *ii)* explore various spectral pre-processing techniques for efficient analysis and mitigation of undesired variations due to hand sanitization, and *iii)* implement a non-parametric two-sample test incorporated with pixel-wise classification to estimate the impact of hand sanitizer and validate the proposed mitigation methods. We identify and investigate a new scientific problem, discuss a novel application of HSI, develop algorithms pertaining to this novel technology and present solutions for mitigating this problem by transforming the original features into various representations in which undesired effects can be attenuated.

The rest of the paper is structured as follows: Section 2 provides a background on hyperspectral imaging, Section 3 summarizes the proposed non-parametric two-sample test based on pixel-wise classification, Section 4 describes the data collected through this study and presents the experimental results, and Section 5 draws our final conclusions.

2. Fingers in Hypercubes

Electromagnetic radiation (EMR) is energy in the form of electromagnetic waves [5]. Substances interact with EMR in different ways. They absorb, reflect, or transmit various wavelengths of EMR differently. Light entering biological tissue undergoes multiple scattering and absorption events as it propagates across the tissue. The penetration depth of light into biological tissues depends on how strongly the tissue absorbs light. Finger's skin is usually characterized by varying curves from region to region which causes diversity in reflecting the light. Fig. 1(a) shows the infrared view of a sample finger hypercube.

Hyperspectral images, also known as hypercubes or datacubes, are three-dimensional data structures, containing two spatial dimensions (X-Y) and one spectral dimension (Z) [1]. One of the most important challenges with hyperspectral imaging is the extraction of useful information from the high dimensional data (hypercube) containing noise and redundant information. HSI enables the simultaneous acquisition of hundreds of spectral wavelengths for each image pixel. While this detailed spectral information increases the possibility of more accurate discrimination, it makes the volume of the feature space enormous. High-dimensional hyperspectral data contains redundant information that needs denoise analysis [6]. In addition to the spectral data, the spatial information obtained from hyperspectral data needs to be utilized to the maximum extent *i.e.*, fusion of spectral and spatial data for developing more robust models. Critical aspects also involved in the processing of hyperspectral images include object segmentation, change in illumination and environmental factors, and heterogeneity of samples. The radiance reaching the sensor is dominated by the solar energy reflected from the objects, and it is proportional to the directional reflectance of the object's surface material. Variability in spectral signatures is due to extrinsic factors (e.g., illumination) and intrinsic factors (e.g., differences in constituent chemicals' concentrations).

Finger hypercubes may exhibit significant differences in the spectra due to physical variations such as sample heterogeneity and uneven surface. These unwanted effects result in additive, multiplicative and wavelength-dependent effects. Typically, wavelength-dependent scattering appears as baseline shifts, tilt or a curvature scaling variation. Huang *et al.* discussed pre-processing techniques that perform scatter correction and reduce spectral baseline shifts could make the model robust to testing data from unseen subjects [7]. Vision properties may be affected by the presence of specular shadow which produces darker regions. These regions act like black objects and lead to absorption of light that could compromise the detected spectrum. Fig. 1(b) illustrates the outcome of a K-mean analysis with K=3 over 300 bands. Ideally, a finger surface must be relatively flat and reflect light evenly. However, the performed clustering highlights that the image can be divided into three groups: background, finger skin, and shadow area. Therefore, the Region of Interest (ROI) is chosen to avoid the uneven reflective area in the finger due to lighting conditions, which helps discard pixels in the shadow area.

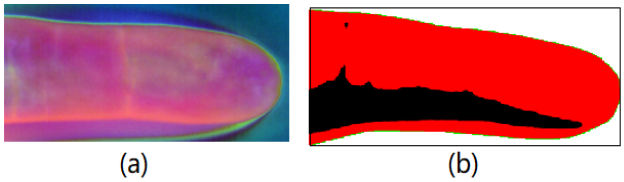

Figure 1. (a) Infrared view of a finger hypercube, (b) K-mean clustering with k=3.

The ROI is obtained through global thresholding and Otsu's method. The selected ROI area is 10x10 pixels around the distal phalanx part of the finger, which is the distal or third of the three bones in each finger when counting from the hand to the tip of the finger. The pixel-wise methods classify an image without using contextual information; thus, the hyperspectral data is considered as an unordered list of spectral vectors where the spatial coordinates are arbitrarily shuffled [8]. Within ROI, each pixel can be viewed as a 1-D array of 300 wavelength values that could be shuffled arbitrarily for computing the arithmetic mean spectrum. This unfolds the hypercube which consists in rearranging the spectra from three dimensions to a matrix with two dimensions. The ROI extracted from each hypercube is then transformed by various spectral pre-processing techniques. Both transformed hypercubes and original spectra are then used for independently training various classifiers.

Fig. 2 shows the mean spectra of the fingerprints collected from the same individual before and after sanitation.

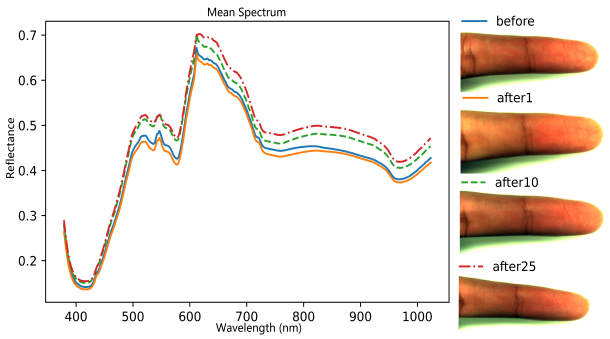

Figure 2. Samples of unfolded finger hypercubes before and after sanitization: the mean spectra of ROI are displayed on the left, with corresponding RGB images of fingers shown on the right.

3. The Proposed HSI-adapted Classifier-based Two-Sample Test

We carry out an HSI-adapted non-parametric classifier-based two-sample test (HSI-C2ST) to determine whether two spectral signals in input are similar or not. C2ST has been proven to be effective in the presence of high dimensional data [9, 10]. In this work, this statistical approach helps understanding how the sanitizer interacts with the finger skin's biochemicals. The architecture of the proposed framework is illustrated in Fig. 3.

The spectral signature of the original data is assumed to follow a distribution $z(t)$, while the spectra obtained from sanitized data follow a distribution and $z(t+k)$, where k indicates the temporal unit expressed in minutes with values in the range 1, 10, 25 [11]. The null hypothesis is that the two signals come from the same distribution, see Eqn. 1; while, the alternative hypothesis is that those two signals belong to different distributions, as indicated in Eqn. 2.

$$H_0 : z(t) = z(t+k) \tag{1}$$

$$H_1 : z(t) \neq z(t+k) \tag{2}$$

C2ST is conducted by training a binary classifier to distinguish between samples $z(t)$ and those in $z(t+1)$. We test whether the null hypothesis is true. Let $z(t)_i = [z(t)_1, z(t)_2, ...z(t)_n]$ denote the set of samples from before $z(t)$, i = 1, $\dots n$. Let $z(t+k)_i = [z(t+k)_1, z(t+k)_2, ...z(t+k)_m]$ denote the set of samples after k mins of applying hand sanitizer $z(t+k)$, i = 1, $\dots m$. A binary classifier $f : \{z_t, z_{t+k}\} \rightarrow [0,1]$ is trained on $Data_{train}$ and the classification accuracy is computed on $Data_{test}$. Given l being the prediction, $f[z(t)_i]$ expresses an estimate of the conditional probability distribution $p(l_i = 1|z(t)_i)$. The decision about accepting or rejecting the null hypothesis is made based on the statistical $\hat{p}$-value associated with the proposed HSI-C2ST, see Eqn. 3 [10].

$$\hat{p} = \frac{1}{n_{test}} \sum_{[z(t)_i, z(t+k)_i] \in Data_{test}} \mathbb{I}\left[\mathbb{I}\left(f\left(z(t)_i\right) > \frac{1}{2}\right) = l_i\right] \tag{3}$$

where $\mathbb{I}$ is the binary classifier, and $n_{test} = |Data_{test}|$ denotes the size of the testing set. If $z(t)$ and $z(t+k)$ follow the same distribution, the accuracy of the classifier is expected to be near chance-level (50%). Let $Model_k$ be the k^{th} classifier trained using observed data $z(t)$ and $z(t+k)$, with k in the range 1, 10, 25. The k^{th} model is built by training it on data that is not pre-processed and sampled at both t=0 and t=k.

Various state-of-the-art algorithms including Support Vector Machines (SVM), Random Forest (RF), and Partial least squares discriminant analysis (PLS-DA) are pixel-wisely trained in the HSI spectral domain and incorporated into the statistical test. HSI-SVM carries out a non-linear pixel-wise classification based on the full spectral information which is robust to the spectral dimension of hyperspectral images [12]. HSI-RF uses several decision tree models built on different sets of bootstrapped features [13]. HSI-PLSDA combines dimensionality reduction and discriminant analysis and is especially applicable to modeling high dimensional data. This algorithm can deal with multicollinearity issues in near-infrared (NIR) spectra, which occurs when spectra are highly correlated [14].

3.1. Pre-processing to Minimize the Impact

The three models $Model_k$ are also trained on pre-processed data to investigate mitigation. Pre-processing hyperspectral data allows the removal of unwanted variations that might impair the interpretation while preserving chemically relevant information [15]. This step is essential when HSI is applied to human fingers due to variability in shape, skin color, temperature, and skin's biochemical content such as sweat metabolites across individuals. Furthermore, random noise and light scattering resulting from variable physical sample properties or instrumental effects can be attenuated.

In this work, we explore pre-processing methods such as Savitzky–Golay first-order derivatives (SG), and multiplicative signal correction (MSC), and standard normal variate (SNV) transformation with detrend spectra (DS). These methodologies are summarized as follows. SG is a derivative filter that smooths the data and increases its precision without distorting the signal tendency, thus preserving the original shape and features. It is used to resolve peak overlap, and eliminate linear baseline drift between samples [16].

SNV normalizes the spectra by subtracting its own mean and dividing it by its own standard deviation [17]. After applying SNV, each centered spectrum will have a mean of 0 and a standard deviation of 1, which makes all the spectra comparable in terms of intensities (or absorbance level). It removes slope variation, corrects light scattering effects, and reduces differences in intensity. DS eliminates wavelength-dependent scattering effects, *i.e.*, variation in curvilinearity between the spectra and baseline shifting. This correction is used after SNV to eliminate trends in spectroscopic data and enable the algorithm to focus on the spectrum fluctuations analysis [18].

MSC is obtained by regressing a measured spectrum against a reference spectrum and correcting the measured spectrum based on the slope and intercept of this linear fit [7]. This method has been proven to be effective in minimizing baseline offsets and multiplicative effects.

Examples of transformed spectra are shown in Fig. 4.

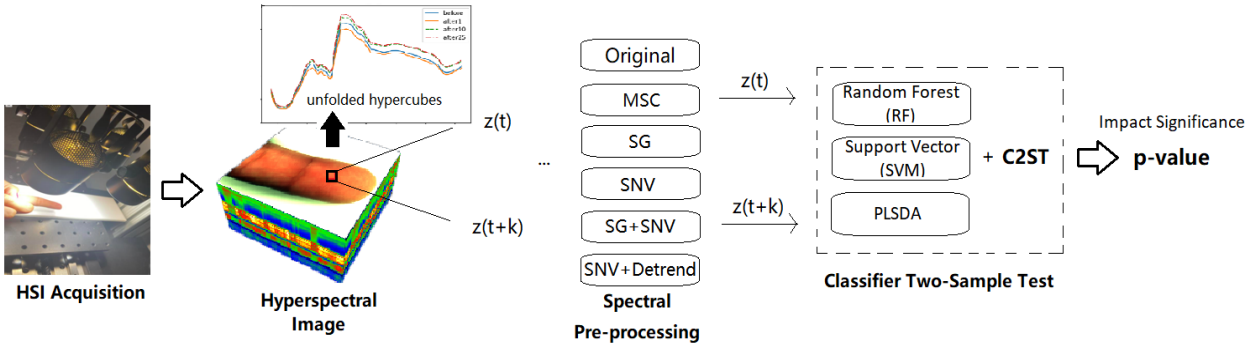

Figure 3. Architecture of the proposed framework: the finger is positioned under the camera as the hyperspectral image is acquired contactless. z(t) and z(t+k) are the sample distributions obtained before and after 1 min of applying hand sanitizer, respectively. To execute the proposed HSI-C2ST, a classifier is trained using a data set balanced between z(t) and z(t+k).

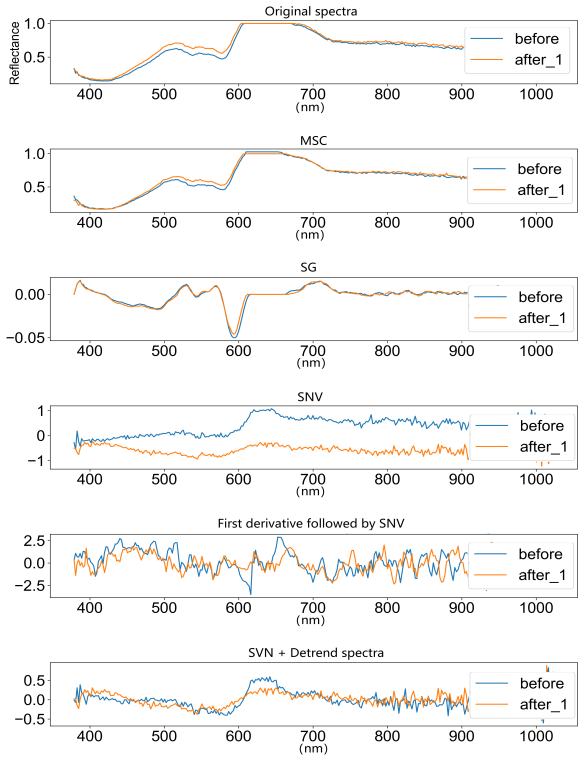

Figure 4. Examples of transformed spectrum: spectra before and after 1 min of applying hand sanitizer indicated by the blue (before) and orange (after_1) curve.

4. Experimental Results

4.1. Dataset

The data used for the experiments is a subset of the GMU CSIS Finger Hypercubes Sanitization with Demographics (FHSD) database [19]. The images used for this study pertain to 50 individuals of different age groups and ethnicities. Individuals with known health issues, or under hormone treatment were not eligible for this study. We also excluded individuals with open wounds/cuts on their hands due to the burning sensation that is caused by the hand sanitizer. The images were acquired by using the Resonon hyperspectral camera PIKA L featured by a spectral range of 378nm to 1023nm, 300 spectral channels. For each individual, four hypercubes were collected: *1)* before applying hand sanitizer, *2)* after 1 min, *3)* after 10 mins and *4)* after 25 mins. Subjects applied themselves a single pump of 3 ml of Purell hand sanitizer by GOJO, which contains 70% ethanol. A 10x10 ROI was extracted from each hypercube, with a total of 100 pixels, each containing 300 spectral bands.

The protocol for the data collection was designed to reproduce a scenario in which individuals are unable to wash their hands right before the interaction with the HSI system.

4.2. Performance Evaluation

The classifiers were trained using 50% of the available data and tested on the remaining 50%. Subjects were mutually exclusive between training and testing to validate that the classifier detects the variations due to the hand sanitizer instead of finger properties (e.g., skin color, lighting condition, temperature) specific to an individual. Furthermore, we also introduced the repeated random sub-sampling validation, also referred to as Monte Carlo cross-validation (MCCV) [20]. We created 20 iterations on random splits of the dataset into 50% for training and 50% for testing. For each such split, the model is fit to the training data, and predictive accuracy is assessed using the testing data. Table 1 reports the average accuracy and p-value over 20 iterations.

The performance is also depicted using the Receiver Operating Characteristic (ROC) curve.

4.3. Results

Table 1 reports the difference between the spectra before and after applying hand sanitizer as investigated by C2ST. A small p-value associated with the C2ST indicates that there is a significant difference among the spectra being analyzed,

which occurs when models are trained by using original spectra without pre-processing. Table 1 also reports the classification performance for the different pre-processing techniques under study. We can see that the accuracy ranges between 40% and 60%. This poor performance suggests that there may be no impact of hand sanitizer on spectral signals when these are appropriately pre-processed. This result is reinforced in Fig. 5 that illustrates the ROC curves for the PLS-DA classifier. A similar trend was found for different classifiers as well. After pre-processing, the p-value becomes significantly greater than 0.05 suggesting that there is no evidence to further support that there is a sanitizer's impact when proper pre-processing is applied to spectrum data.

We also observed that spectral pre-processing approaches applying baseline corrections, (i.e., SG and Detrend) outperform other methods that exclusively focus on light scattering effects. SG, SG+SNV, and SNV+Detrend reached an accuracy much closer to the chance level (50%); thus, C2ST rejected the null hypothesis. SG is expected to reduce baseline shift, MSC to reduce the multiplicative effect, SNV to mitigate light scattering effects, and Detrend to minimize variations in curvilinearity between the spectra and the baseline shift. As result, proper pre-processing techniques can help in finding the transformed feature space where the impact of heterogeneous samples is not significant.

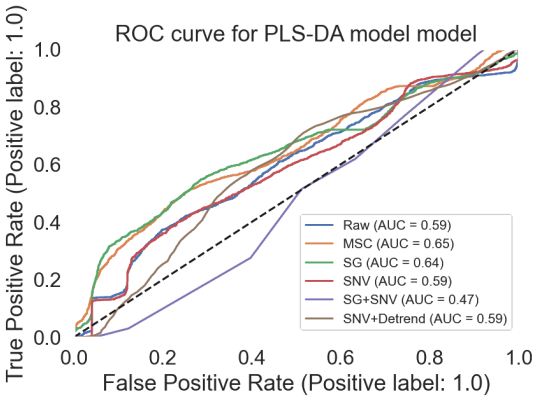

Figure 5. ROC curve for Partial Least Squares-Discriminant Analysis (PLS-DA) with n-components = 100.

Incorporating in the test additional classifiers is expected to have similar results using the pre-processing techniques under study. Furthermore, exploring deep nets would involve image classification rather than the pixel-wise approach that we implemented in this work.

5. Conclusions

Since the COVID-19 pandemic, the use of hand sanitizer has become much more popular given the guideline by medical experts. We investigate whether hand sanitizer impacts hyperspectral images of human fingers. The proposed study analyses the spectral signature pixel-wise. These spectra were evaluated through the Classifier Two-Sample Test (C2ST) adapted to HSI, as well as by using various pre-processing techniques before training. The proposed framework is general and may involve traditional classifiers adapted to HSI domain as well as deep learning. For the experiments, we used finger hypercubes collected in our lab from 50 individuals. Results do not show evidence of significant impact from hand sanitizer only when the signals are appropriately pre-processed in particular through methods that perform baseline correction.

In future work, we will: *i)* extend this study on a larger database, *ii)* investigate additional statistical tests and classification algorithms including deep learning formulations for HSI, *iii)* explore domain adaptation techniques, and *iv)* train generative models. We are also planning to incorporate the protocol for the data collection scenarios where people are asked to wash their hands for a certain number of seconds by using specific anti-bacterial soaps before applying hand sanitizer. This will validate our study also the impact when washing is available to the individuals.

6. Acknowledgements

This research was supported in part by Award No. 2036151 awarded by the National Science Foundation (NSF), division of Chemical, Bioengineering, Environmental and Transport Systems (CBET). The opinions, findings, and conclusions or recommendations expressed in this publication are those of the authors and do not necessarily reflect those of the US National Science Foundation (NSF).

References

[1] G. Reed, K. Savage, D. Edwards, and N. N. Daéid, "Hyperspectral imaging of gel pen inks: an emerging tool in document analysis.," *Science & justice : journal of the Forensic Science Society*, vol. 54 1, pp. 71–80, 2014. 1, 2

[2] P. Hazarika, S. M. Jickells, and D. A. Russell, "Rapid detection of drug metabolites in latent fingermarks.," *The Analyst*, vol. 134 1, pp. 93–6, 2009. 1

[3] P. Prajapati, H. Desai, and C. Chandarana, "Hand sanitizers as a preventive measure in covid-19 pandemic, its characteristics, and harmful effects: a review," *Journal of the Egyptian Public Health Association*, vol. 97, 2022. 1

[4] P. Prajapati, H. Desai, and C. Chandarana, "Hand sanitizers as a preventive measure in covid-19 pandemic, its characteristics, and harmful effects: a review," *Journal of the Egyptian Public Health Association*, vol. 97, Feb 2022. 1

[5] M. Kamruzzaman and D. Sun, "Introduction to hyperspectral imaging technology," 2016. 2

[6] D. Saha and A. Manickavasagan, "Machine learning techniques for analysis of hyperspectral images to determine

Table 1. The average accuracy for each classifier and pre-processing technique is reported over 20 iterations. P-value is obtained through classifier two-sample test (C2ST), where bolded numbers indicate p-value < 0.05.

		Avg. Accuracy			C2ST P-value		
Pre-processing	Algorithm	z(t+1)	z(t+10)	z(t+25)	z(t+1)	z(t+10)	z(t+25)
Original	RF	61.44%	59.37%	57.03%	**8.75E-04**	**0.004**	**0.028**
	SVM	41.12%	57.85%	43.82%	**6.06E-04**	**0.001**	**0.002**
	PLSDA	57.24%	59.84%	45.61%	**0.002**	**0.007**	0.061
MSC	RF	59.06%	59.10%	57.66%	**0.002**	**0.002**	**0.03**
	SVM	57.27%	55.61%	44.23%	**0.038**	0.051	**0.029**
	PLSDA	59.20%	60.04%	58.20%	**0.001**	**3.60E-03**	**0.009**
SNV	RF	42.70%	56.12%	58.88%	**0.012**	**0.043**	**0.001**
	SVM	65.15%	61.22%	57.61%	**1.04E-05**	**1.79E-04**	**0.002**
	PLSDA	54.50%	58.84%	58.17%	**0.009**	**0.032**	**0.038**
SG	RF	53.85%	48.98%	51.96%	0.387	0.090	0.121
	SVM	53.26%	50.88%	50.10%	0.167	0.760	0.903
	PLSDA	51.51%	47.67%	53.12%	0.334	0.269	0.098
SG+SNV	RF	51.20%	50.61%	50.11%	0.855	0.912	0.891
	SVM	49.98%	51.77%	49.54%	0.893	0.762	0.714
	PLSDA	49.75%	51.29%	50.67%	0.337	0.514	0.876
SNV+Detrend	RF	50.44%	51.06%	52.12%	0.869	0.564	0.304
	SVM	50.72%	50.48%	51.47%	0.598	0.891	0.214
	PLSDA	51.14%	49.98%	50.99%	0.427	0.934	0.248

quality of food products: A review," *Current Research in Food Science*, vol. 4, pp. 28 – 44, 2021. 2

[7] J. Huang, S. Romero-Torres, and M. Moshgbar, "Practical considerations in data pre-treatment for nir and raman spectroscopy," *American Pharmaceutical Review*, 2010. 2, 3

[8] D. Valencia, A. J. Plaza, P. Martínez, and J. Plaza, "On the use of cluster computing architectures for implementation of hyperspectral image analysis algorithms," *10th IEEE Symposium on Computers and Communications (ISCC'05)*, pp. 995–1000, 2005. 2

[9] K. P. Chwialkowski, A. Ramdas, D. Sejdinovic, and A. Gretton, "Fast two-sample testing with analytic representations of probability measures," *Advances in Neural Information Processing Systems*, vol. 28, 2015. 3

[10] D. Lopez-Paz and M. Oquab, "Revisiting classifier two-sample tests for gan evaluation and causal discovery," 2016. 3

[11] Y. Liu, C.-L. Li, and B. Poczos, "Classifier two sample test for video anomaly detections," *In BMVC*, 2018. 3

[12] Z. He, Y. Shen, M. Zhang, Q. Wang, Y. Wang, and R. Yu, "Spectral-spatial hyperspectral image classification via svm and superpixel segmentation," *2014 IEEE International Instrumentation and Measurement Technology Conference (I2MTC) Proceedings*, pp. 422–427, 2014. 3

[13] R. Vinayakumar, K. P. Soman, P. Poornachandran, S. Akarsh, and M. Elhoseny, "Improved dga domain names detection and categorization using deep learning architectures with classical machine learning algorithms," *Advanced Sciences and Technologies for Security Applications*, 2019. 3

[14] E. Ivorra, J. Girón, A. J. Sánchez, S. Verdu, J. M. Barat, and R. Grau, "Detection of expired vacuum-packed smoked salmon based on pls-da method using hyperspectral images," *Journal of Food Engineering*, vol. 117, pp. 342–349, 2013. 3

[15] R. J. Barnes, M. S. Dhanoa, and S. J. Lister, "Standard normal variate transformation and de-trending of near-infrared diffuse reflectance spectra," *Applied Spectroscopy*, vol. 43, pp. 772 – 777, 1989. 3

[16] G. L, N. S.-A., and R.-K. T. J., "Glidertools: A python toolbox for processing underwater glider data.," 2019. Frontiers in Marine Science, 6(December), 1–13. https://doi.org/10.3389/fmars.2019.00738. 3

[17] G. J. McLachlan, S. I. Rathnayake, and S. X. Lee, "Comprehensive chemometrics: chemical and biochemical data analysis," 2020. 3

[18] M. Oravec, L. Gál, and M. eppan, "Pre-processing of inkjet prints nir spectral data for principal component analysis," *Acta Chimica Slovaca*, vol. 8, pp. 191 – 196, 2015. 3

[19] E. M. Sriram Sai Sumanth, "A novel demographic-based time-series database of finger hypercubes before and after hand sanitization," in *2022 26th International Conference on Pattern Recognition (ICPR)*, 2022. https://github.com/cysber-CSIS. 4

[20] Q.-S. Xu and Y.-Z. Liang, "Monte carlo cross validation," *Chemometrics and Intelligent Laboratory Systems*, vol. 56, no. 1, pp. 1–11, 2001. 4